Int J Thermophys (2008) 29:1041–1051
DOI 10.1007/s10765-008-0406-0

AC-Mode Short-Wavelength IR Radiation Thermometers for Measurement of Ambient Temperatures

G. P. Eppeldauer · H. W. Yoon

Published online: 18 March 2008

Abstract Recent improvements in the fabrication of short-wave infrared (SW-IR) quantum detectors have opened a new era in radiation thermometry. Ambient and higher temperatures can be measured with low uncertainties using thermoelectrically (TE) cooled extended-InGaAs (E-IGA) and short-wave photovoltaic-HgCdTe (SW-MCT) detectors. Since these detectors have low cut-off wavelengths (2.5 µm and 2.8 µm, respectively), they do not respond past cut-off and are less sensitive to the background infrared radiation, resulting in orders of magnitude lower background noise than traditional broad-band infrared detectors such as cryogenically cooled quantum detectors or thermal detectors. At the same time, the cut-off is far enough in the infrared to obtain a large enough signal from the source of interest. Because of the low detector cut-off wavelength, traditional glass-based optics can be used in the radiation thermometers. A chopper-produced alternating-current (AC) signal was used to measure low temperatures by separating the AC signal from the background-radiation-produced direct-current (DC) signal and its fluctuations. Design considerations and characteristics of a newly developed SW-IR radiation thermometer are discussed. A noise-equivalent temperature difference (NETD) of <3 mK for a 50°C blackbody was measured. At the human body temperature of 36°C, the obtained NETD of ~ 10 mK indicates that these detectors can be used in non-contact temperature measurements to replace thermopile- or pyroelectric-based radiation thermometers.

Keywords Ambient temperatures · Infrared · Input optics · NETD · NEP · Noise · Optical radiation · Radiance · Radiation thermometer · Responsivity · Non-contact body temperature

G. P. Eppeldauer (✉) · H. W. Yoon
Optical Technology Division (844), National Institute of Standards and Technology,
100 Bureau Drive, Stop 8441, Gaithersburg, MD 20899-8441, USA
e-mail: george.eppeldauer@nist.gov

1 Introduction

Traditional infrared detectors, such as cryogenically cooled quantum detectors and thermal detectors, operate in a background-limited mode because of their long cut-off wavelengths. In this mode, the background radiation is orders of magnitude larger than the target radiation. In addition, the high background-radiation-produced DC signal is not stable and has a large noise component. The signal to be measured is usually AC, to separate it from the DC background signal. However, the large noise component of the DC background signal will dominate the output noise of the radiometer unless the background signal is significantly reduced.

Furthermore, ambient-temperature thermal detectors (e.g., thermopiles or pyroelectric detectors) have low responsivities and, thus, high noise-equivalent powers (NEP). They need large signals (sufficient thermal radiation within the detector system band-pass) to obtain reasonable signal-to-noise ratios at the output of the radiometers. In many applications, large thermal radiation to be measured is not available, and the signal (photocurrent) gain in the radiometers cannot be increased to improve the poor signal-to-noise ratios. Both the above limitations are apparent in current designs of radiation thermometers for measuring human body temperatures. They are prone to drift from changes in the immediate thermal environment around the detector and also are not capable of transferring a temperature scale to within ± 0.2°C from 32°C to 45°C [1].

We describe the development of a short-wave infrared (SW-IR) radiation thermometer that can be used as a transfer standard to measure low-temperature radiometric sources with low uncertainty and high stability. The design issues and the characteristics of this thermometer are discussed here, and we show that cryogenic, quantum detector-based radiation thermometer performance can be achieved with thermo-electrically cooled SW-IR radiation thermometers.

2 NETD and NEP of Radiation Thermometers

The noise-equivalent temperature difference (NETD) and the noise-equivalent power (NEP) of a radiation thermometer are noise figures of merit that are closely related. The NETD shows the sensitivity (temperature resolution) of a thermometer while the NEP is used to optimize the detectivity of a radiation thermometer.

The NETD is determined when the thermometer measures the radiation from a stable source. In this case, the standard deviation of the measured photocurrent values is divided by the mean of the values to obtain the NETD. The noise-equivalent signal fluctuation $\Delta S/S$ can come from both the emitted radiation and the noise in the output signal of the thermometer. Using the derivative of the Wien approximation,

$$\frac{\Delta S}{S} = \frac{\Delta L}{L} = \frac{c_2}{\lambda}\frac{\Delta T}{T^2} \tag{1}$$

where L is the source radiance, $c_2 = 1.4387752 \times 10^{-2}\ \mathrm{m \cdot K}$, T is the temperature of the source, and λ is the wavelength where the detector is responsive to the broad-band

source radiation (such as a blackbody); the NETD can be equated with the calculated ΔT.

In contrast to the above-suggested NETD measurements, the NEP is measured at zero (dark or blocked) signal, or close to zero signal. The NEP is the ratio of the output noise N to the responsivity R of the radiation thermometer, usually at an electrical bandwidth of 1 Hz;

$$\mathrm{NEP} = \frac{N(\mathrm{output})}{R}. \tag{2}$$

The output noise can be obtained as the standard deviation of the thermometer photocurrent (output voltage per photocurrent-to-voltage gain). The unit of NEP is $\mathrm{W} \cdot \mathrm{Hz}^{-1/2}$. The detectivity D^* of the thermometer (comprising the radiation detector and the preamplifier) can be calculated from the NEP,

$$D^* = \frac{\sqrt{A}}{\mathrm{NEP}}, \tag{3}$$

where A is the active area of the detector. The unit of detectivity is $\mathrm{cm} \cdot \mathrm{Hz}^{1/2} \cdot \mathrm{W}^{-1}$.

In traditional broad-band detector applications, where the background-produced photocurrent is high, the photocurrent-to-voltage gain (a component of R) cannot be increased to high values without saturating the photocurrent-to-voltage converter, but the low R will result in a high NEP. The lower background signal of SW-IR detectors makes it possible to increase the photocurrent-to-voltage gain in the preamplifier of the radiometer.

The NETD of ambient thermal detectors is higher than 0.1 K, which makes them difficult to use for low-uncertainty measurements in many applications, such as for ear thermometers [1]. The responsivity of such detectors, i.e., thermopiles and pyroelectric detectors, is low. For example, the power responsivity of a pyroelectric detector is six orders of magnitude lower than that of InGaAs (including extended-InGaAs) detectors, resulting in six orders of magnitude higher NEP.

Detectors with high responsivity for the SW-IR and low responsivity (high rejection) for the long-wave infrared (LW-IR) should be used to achieve low NEP and NETD in radiation thermometers. In order to obtain maximum responsivity, the shunt resistance of the detector should be maximized and the feedback resistance of the photocurrent-to-voltage converter should be equal to, or higher than, the maximized shunt resistance. Also, the output noise, N, should be minimized.

3 Decrease of Thermometer Output Noise

The output noise of a thermometer can be decreased in a few ways. The dominating noise components are the amplified $1/f$ noise of the current-measuring preamplifier, the resistor (Johnson) noise (which is obtained from the parallel combination of the detector shunt resistance and the feedback resistance of the current meter), and the remaining background noise [2]. These three noise components must be minimized

to achieve low values of NEP. This is in contrast to the dominantly background-noise-limited operational mode of traditional mid-IR and long-IR thermometers.

The $1/f$ noise can be significantly decreased using AC signal measurement techniques. In this case, the signal frequency is much higher than in DC mode measurements. The signal frequency should be selected near the elbow of the $1/f$ noise spectrum of the current-to-voltage converter (preamplifier). A high photodiode shunt resistance can keep the closed-loop voltage gain of the photocurrent-to-voltage converter low [3], resulting in low noise at the output of the radiometer. The noise of the remaining background signal can be further decreased using a metal detector case with a built-in thermoelectric (TE) cooler and a cold field-of-view (FOV) limiter for the detector. The side of the metal can, viewed by the detector, should remain at room temperature to avoid radiating excess heat onto the detector. The achievable signal-to-noise ratio is determined by the performance of the first-stage amplifier (preamplifier), which includes the detector and the current-to-voltage converter. As the noise is electrical bandwidth dependent, it can be further reduced if the AC signal of the radiometer (thermometer) output is measured with a lock-in amplifier that has a large time-constant low-pass filter.

4 Photocurrent Measurement

In order to describe the effects of detector and feedback impedances and noise sources in a photodiode current meter, the equivalent circuit must be discussed. As shown in Fig. 1, a photodiode P can be substituted by an ideal current source (double circle) and parallel-connected shunt resistance R_S and junction capacitance C_J. The photocurrent I_P from photodiode P is converted into a voltage V at the output of the operational amplifier (OA). R is the feedback resistance, and C is the feedback capacitance of the OA. I_{IN} is the input current noise and V_{VN} the input voltage noise of the OA. The resistor noise that originates from the parallel connection of R and R_S is not illustrated here to keep the equivalent circuit simple. The resistor noise will be superimposed on V without any amplification.

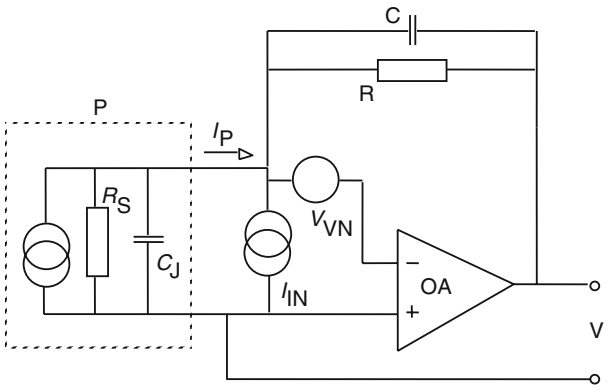

Fig. 1 Equivalent circuit of a photodiode current meter. The photodiode P is denoted by the dotted line

The signal gain (current-to-voltage conversion) is the following:

$$\frac{V}{I_{\mathrm{P}}} = R\left(\frac{1}{1+j\omega RC}\right)\left(\frac{1}{1+G^{-1}}\right) \tag{4}$$

where RC is the time constant produced by the feedback components. It determines the upper frequency roll-off of the signal. G is the loop gain, and it must be large at the signal (i.e., the chopping) frequency to keep the uncertainty of the current-to-voltage gain low. The loop gain (the product of the OA open-loop gain A and the feedback attenuation β) is

$$G = A\beta \tag{5}$$

where $\beta = R_{\mathrm{S}}/(R_{\mathrm{S}} + R)$ at low frequency, i.e., as with DC measurements. High loop gain can be obtained if β is close to unity (its maximum value). To achieve this condition, the shunt impedance, $Z_{\mathrm{S}}(\equiv R_{\mathrm{S}}/1 + j\omega R_{\mathrm{S}}C_{\mathrm{S}})$, must be high at the signal frequency. C_{S} is the shunt capacitance of the photodiode.

The closed-loop voltage gain that determines the amplification of the input noise, offset, and drift at the output of the current-to-voltage converter is the reciprocal of β:

$$A_{\mathrm{V}} = \frac{R_{\mathrm{S}} + R}{R_{\mathrm{S}}} \tag{6}$$

Again, A_{V} can be kept small (close to unity) if the shunt resistance is high relative to the feedback resistance. As with the signal gain above, both G and A_{V} are frequency dependent [4].

When the shunt resistance is high, the feedback resistor of the current-to-voltage amplifier (that determines the signal gain) can be high as well.

The input impedance of the above photocurrent meter can be calculated as the parallel connection of the down-transformed (divided by A) feedback resistor and the up-transformed (multiplied by A) feedback capacitor of the OA:

$$(Z_{\mathrm{I}})^{-1} = \left(\frac{R}{A}\right)^{-1} + \left(\frac{1}{j\omega AC}\right)^{-1} \tag{7}$$

Linear signal gain (response) can be achieved if the short-circuit photocurrent of the photodiode is measured. In this case, the photodiode shunt impedance must be much larger than the input impedance of the current meter;

$$Z_{\mathrm{I}} \ll Z_{\mathrm{P}} \tag{8}$$

The preamplifier should not produce any distortion in the wave shape of the chopped optical signal. This requirement can be achieved if the upper roll-off frequency of the preamplifier is selected high enough:

$$f = \frac{1}{2\pi RC} \tag{9}$$

where RC is the time constant from Eq. 4. In practice, the time constant is tuned by changing C. In addition to affecting the frequency dependence of the signal gain, a change in C will modify the frequency dependence of G and A_V as well. Therefore, these three gains are to be optimized together for the signal (chopping) frequency at all signal-gain selections [3].

5 Second-Stage Lock-in Amplifier

A large signal-to-noise ratio, as the result of the above-discussed first-stage (detector-current meter) optimization, can be further increased using a second-stage lock-in amplifier. The lock-in amplifier makes a phase-sensitive rectification of its AC input signal and filters out signal components at different frequencies other than the chopping frequency (of the optical signal to be measured). The filter of the lock-in amplifier limits the electrical bandwidth around the signal (chopping) frequency. Using a sine-wave measuring lock-in amplifier, only the fundamental frequency component of the AC input signal will be measured. The theoretical reading (conversion factor) of a sine-wave measuring lock-in amplifier is

$$S_1 = \frac{H}{\sqrt{2}}\frac{4}{\pi} = 0.9003H \tag{10}$$

where H is half of the peak-to-peak amplitude of the square wave signal (which is equal to zero when the chopper blocks the radiation). This conversion factor is not always accurate. It can be calibrated against a digital voltmeter (DVM) in the DC mode if the input signal has a large signal-to-noise ratio. If the chopper is stopped, the DVM reading will be $S_2 = 2H$. The real correction factor will be the ratio of the lock-in amplifier reading to the DVM reading.

In many cases, the frequency-dependent responsivity of a detector-preamplifier standard is measured during its calibration and the DC responsivity is reported. When this detector-preamplifier standard is used in an application where the chopper and the lock-in amplifiers are different, the frequency-dependent responsivity is measured again with these different instruments and the DC responsivity is extended to the signal frequency of this application using the measured curve. Using the theoretical conversion factor S_1, the DC responsivity is $2/0.9003 = 2.22$ times higher than the value measured by the lock-in amplifier.

6 Design of Sensitive Radiation Thermometers

The wavelength interval for a sensitive radiation thermometer should be properly selected to obtain high ratios of signal from the target relative to that of the background. Figure 2 shows different blackbody radiance curves for target temperatures ranging from −63 to 850°C. The graph shows that at long wavelengths the target-signal-to-background-signal (contrast) ratios are much smaller than in the atmospheric window between 2 µm and 2.5 µm where the SWIR detectors operate. The vertical lines show

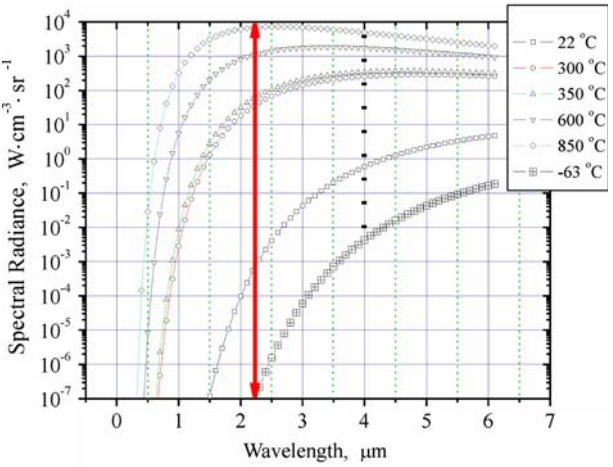

Fig. 2 Planck radiance curves between −63 and 850°C. The target-signal-to-background-signal ratios are shown with vertical lines at 2.25 μm and 4 μm

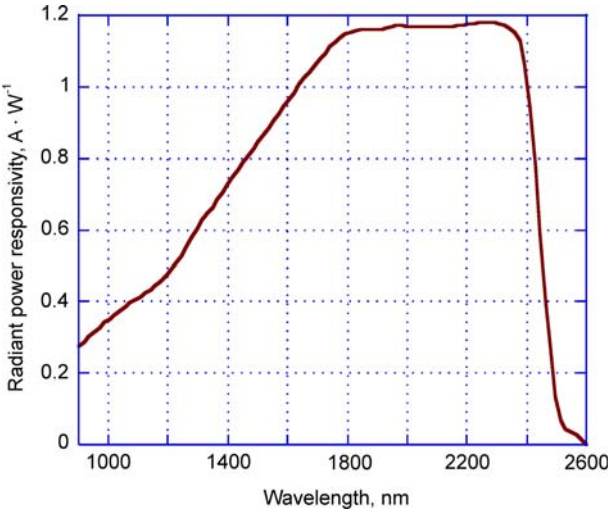

Fig. 3 Spectral power responsivity of an extended-InGaAs detector

orders of magnitude increase in the contrast ratio when the thermometer measures at 2.25 μm instead of 4 μm.

Figure 2 also shows that the target signal at 2.25 μm is about an order of magnitude smaller than at 4 μm or longer. Therefore, detectors with high D* should be selected for the atmospheric window between 2 μm and 2.5 μm. Figure 3 shows the spectral power responsivity of an extended-InGaAs (E-IGA) detector. It can be seen that the responsivity is high in the 2–2.5 μm wavelength range.

Figure 4 shows the wavelength dependence of D* of several high radiometric quality detector-preamplifier units (radiometers), such as Si and InGaAs (near-IR) radiometers

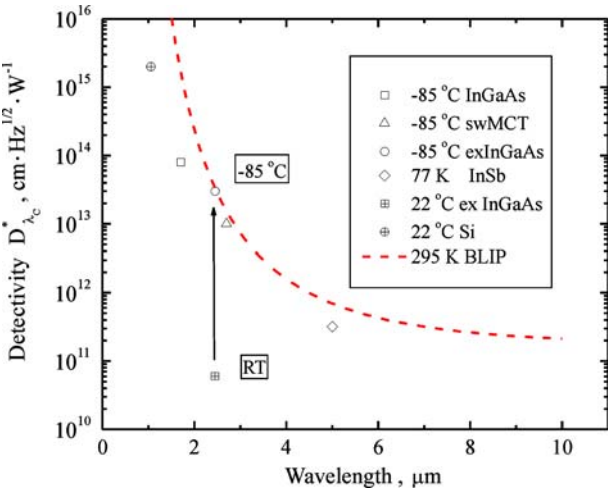

Fig. 4 D* of silicon, near-IR, SW-IR, and mid-IR radiometers with the background-limited power curve at 295 K calculated with an $f/2$ detector FOV and an electrical bandwidth of 0.16 Hz

and different infrared radiometers, including SW-IR such as E-IGA and SW-HgCdTe (SW-MCT), and mid-wave infrared (mid-IR) InSb. The background-limited power (BLIP) curve, which gives the theoretical limit for D* [5], was calculated with an $f/2$ detector field-of-view (FOV) for 295 K background radiation. The graph shows that the D* of a room-temperature E-IGA radiometer was increased by almost three orders of magnitude when the detector was cooled to −85°C. As a result of equalizing the three dominant noise components, the obtained D* value of 3×10^{13} cm · Hz$^{1/2}$ · W^{-1} is very close to the background noise theoretical limit. The SW-MCT radiometer, with a 2.8 μm cut-off, is also very close to the BLIP curve. The D* of an InSb radiometer (with optimized background rejection) is about two orders of magnitude lower. The Si and InGaAs radiometers have very high D* values but they are not suited for detection of objects at ambient temperatures since there is insufficient signal at these wavelengths (the BLIP is $> 10^{18}$ cm · Hz$^{1/2}$ · W^{-1}).

Thermometers with high D* (high responsivity and low noise) can be developed if detectors with high shunt resistance are used. The shunt resistance of a 1-mm-diameter SW-IR detector can be increased to about 10 MΩ from 10 kΩ (at room temperature) when it is cooled to about −70°C or lower [6]. Instead of cryogenic cooling, which is traditionally used for InSb detectors, four-stage thermoelectric (TE) coolers can be used.

7 SW-IR Radiation Thermometer Construction

Using the above design considerations, an experimental radiation thermometer was constructed to determine the NETD as a function of blackbody temperature. Since optical glasses transmit at these wavelengths, regular achromats were used as objective lenses in the prototype shown in Fig. 5. A variable-temperature blackbody set to

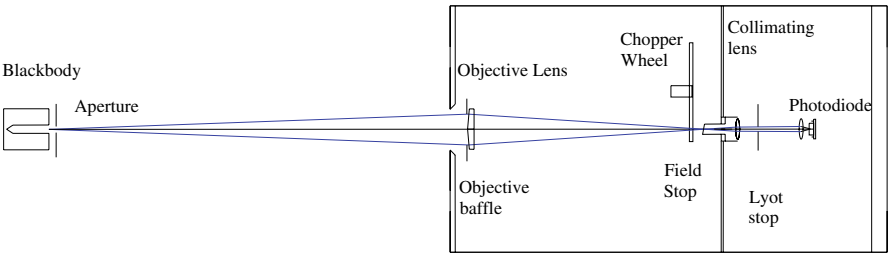

Fig. 5 SW-IR radiation thermometer construction

room temperatures and higher was used as the source of radiation. A 6-mm-diameter target was imaged by the radiation thermometer with a distance of 50 cm between the source aperture and the front of the objective lens. The radiation was imaged onto a field stop with a chopper wheel placed close to the field stop. The radiation was collimated and focused onto a 1-mm-diameter detector with achromats. The detector was under-filled by the image. The extended-InGaAs detector was cooled to −85°C with TE cooling. The detector was attached to a short-circuit photocurrent meter built with a low-noise operational amplifier. The Lyot stop [7] serves as the aperture stop behind the field stop. Due to the low-scatter objective and the Lyot stop, the thermometer has excellent out-of-field rejection that enables internal chopping.

8 NEP and NETD Measurement Results

The output total noise voltage was measured versus signal-gain selections for a 3-mm (3 MΩ shunt resistance) extended-InGaAs photodiode current meter. The temperature of the detector was controlled to −85°C using a four-stage TE cooler. The noise equivalent current (NEC) is equal to the measured total noise voltage divided by the current-to-voltage gain (the value of the feedback resistor). The total noise voltage was measured by a lock-in amplifier attached to the output of the photocurrent meter. The chopping frequency was 7.5 Hz and the integrating time constant of the lock-in amplifier was 1 s. The signal source was a 314°C blackbody located about 50 cm from the radiometer. The NEP was calculated as the ratio of the NEC to the detector (peak) power responsivity of $1.2\,\mathrm{A}\cdot\mathrm{W}^{-1}$ (at 2 μm). The NEC and NEP results are shown on the two y-axes of Fig. 6. The measured data points are connected by straight lines for better illustration. The graph shows that a NEP = 15 fW was obtained with the 1 s integration time constant. The NEP of this SWIR detector is more than six orders of magnitude lower than the 50–100 $\mathrm{nW}\cdot\mathrm{Hz}^{-1/2}$ NEP of pyroelectric detectors. The 15 fW (obtained with 1 s time constant) NEP (and the related output signal-to-noise ratio) could not be improved at the $10^8\ \mathrm{V}\cdot\mathrm{A}^{-1}$ and $10^9\ \mathrm{V}\cdot\mathrm{A}^{-1}$ signal gains relative to the $10^7\ \mathrm{V}\cdot\mathrm{A}^{-1}$ selection where the shunt resistance is roughly equal to the feedback resistance. At gain selections of $10^7\ \mathrm{V}\cdot\mathrm{A}^{-1}$ and higher, the constant 3 MΩ shunt resistance dominates the resistor noise. The $10^8\ \mathrm{V}\cdot\mathrm{A}^{-1}$ and higher signal gains should be utilized only with higher than 3-MΩ shunt-resistance detectors because the loop gain decreases and there is no further signal-to-noise advantage. Higher shunt resistances

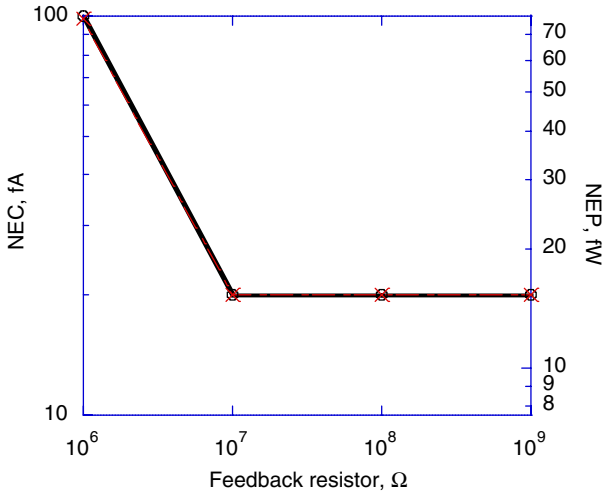

Fig. 6 NEP (right-Y) and NEC (left-Y) of a 3-MΩ shunt-resistance E-IGA photodiode current meter at a lock-in amplifier integrating time constant of 1 s

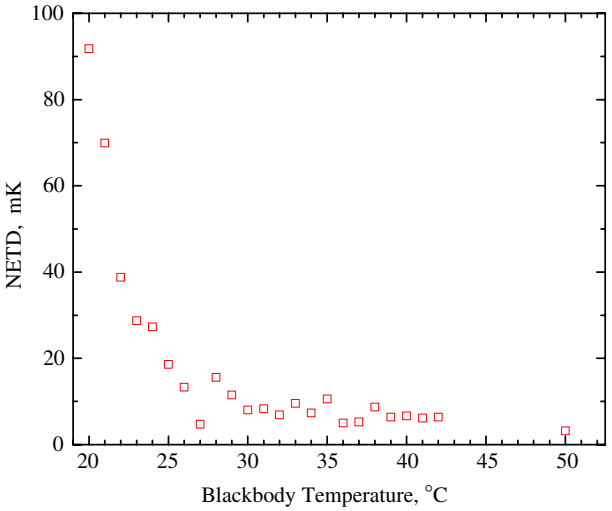

Fig. 7 NETD of the experimental radiation thermometer versus target temperature

of 10–15 MΩ were measured for 1-mm-diameter E-IGA and SW-MCT detectors. In these cases, the NEP can be further decreased.

At a blackbody temperature of 50°C, a NETD of <3 mK was obtained from the standard deviation of the temperature measurements taken with an electrical bandwidth of 0.16 Hz.

The NETD plotted as a function of the blackbody temperature is shown in Fig. 7. The NETD increases rapidly as the target temperature becomes comparable to the chopper-wheel temperature, but at the human-body temperature of 36°C, the NETD

is ∼10 mK. These results demonstrate that the NETD is comparable to that of InSb detectors for blackbody temperatures > 25°C without the need for cryogenic cooling.

9 Conclusions

Thermoelectrically cooled SW-IR detectors attached to noise-optimized photocurrent meters can be incorporated into radiation thermometers utilizing traditional achromats to measure objects at human body temperatures. The SW-IR thermometers operate in the 2–2.5 μm atmospheric window where the target signal is lower than in the mid-IR. However, the target-signal-to-background-signal ratio is orders of magnitude higher than in the mid-IR or long-IR ranges. The NEP of the SW-IR thermometers is more than six orders of magnitude lower than that of pyroelectric thermometers. An optically and electronically optimized SW-IR radiation thermometer was designed, built, and tested. Regular glass input optics were used, and the incident radiation was chopped. The achieved NEP was 15 fW (with 1 s integration time constant) and the NETD increased from 3 mK at 50 °C to 10 mK at 36°C. While standard-quality radiation thermometers with high sensitivity are not presently available, the described SW-IR thermometer can measure ambient temperature sources, such as water-bath or tin-point blackbodies, with very low uncertainties. With this suggested radiation thermometer standard, the temperature of the human body can be measured with a NETD of 10 mK, which is about an order of magnitude improvement over existing ear thermometers. These results indicate that transfer standard radiation thermometers for measurements of human body temperatures can be constructed without utilizing cryogenic or thermal detectors.

References

1. I. Pusnik, E. van der Ham, J. Drovsek, Physiol. Meas. **25**, 699 (2004)
2. G.P. Eppeldauer, A.L. Migdall, L.M. Hanssen, Metrologia **35**, 485 (1998)
3. G.P. Eppeldauer, in NIST Technical Note 1438 (2001)
4. G.P. Eppeldauer, J. Res. NIST **103**, 153 (1998)
5. A. Rogalski, K. Chrzanowski, Opto-Electron. Rev. **10**, 111 (2002)
6. H.W. Yoon, M.C. Dopkiss, G.P. Eppeldauer, SPIE Proc. **6297**, 629703-1–629703-10 (2006)
7. H.W. Yoon, D.W. Allen, R.D. Saunders, Metrologia **42**, 89 (2005)